RSC Advances

ROYAL SOCIETY OF CHEMISTRY

www.rsc.org/advances

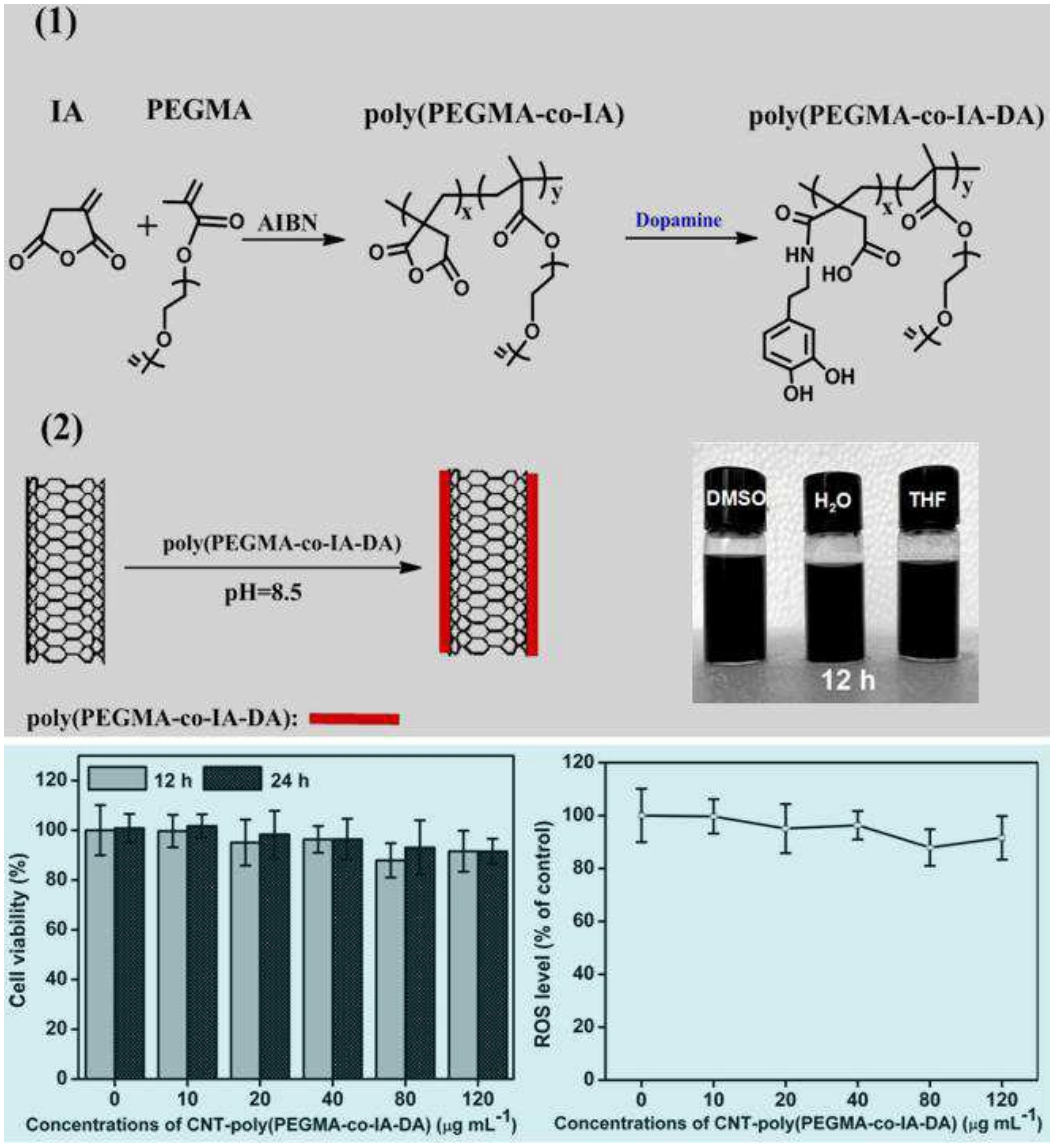

A novel method for preparation of water dispersible and biocompatible carbon nanotubes via mussel inspired PEGylation has been developed for the first time.

Cite this: DOI: 10.1039/c0xx00000x

www.rsc.org/xxxxxx

Full Paper

Mussel Inspired Preparation of High Dispersible and Biocompatible Carbon Nanotubes

Qing Wan[a], Jianwen Tian[a], Meiying Liu[a], Guangjian Zeng[a], Zhen Li[b], Ke Wang[b], Qingsong Zhang[b], Fengjie Deng[a,*], Xiaoyong Zhang[a,*] and Yen Wei[b,*]

Received (in XXX, XXX) Xth XXXXXXXXX 200X, Accepted Xth XXXXXXXXX 200X
DOI: 10.1039/b000000x

The biomedical applications of carbon nanotubes (CNTs) have been intensively investigated. However, poor water dispersibility and obvious toxicity of pristine CNTs are still two major issues for their biomedical applications. Although great efforts have been devoted to solving these problems, a simple and effective strategy for preparation of CNTs with high water dispersibility and desirable biocompatible is still of great research interest. Herein, surface modification of CNTs with a biocompatible polymer polyethylene glycol (PEG) via mussel inspired strategy has been developed. The dispersibility as well as biocompatibility of these PEGylated CNTs (named as CNT-poly(PEGMA-co-IA-DA)) was subsequently investigated. These PEGylated CNTs showed remarkable enhancement of dispersibility in aqueous and organic solvents. More importantly, as evidenced by cell viability and reactive oxygen species results, these PEGylated CNTs showed negative toxicity toward cancer cells. Therefore the PEGylated strategy described in this work can provide a general platform for fabrication of multifunctional biomaterials for various biomedical applications because of the advantages of mussel inspired chemistry and excellent properties of PEGylated materials.

1. Introduction

As a type of one-dimensional carbon nanomaterials, carbon nanotubes (CNTs) have attracted great research interest since their first discovery in 1991.[1] Owing to their unique structure and extraordinary physicochemical properties, CNTs have been extensively explored for different applications ranging from nanocomposite filler, field emission displays, energy storage and conversion, biosensor and drug delivery carries *et al*.[2-9] Especially, the biomedical applications of CNTs have been intensively investigated recently for their large specific surface areas and high cell membrane penetration capability.[10, 11] It has been demonstrated that various active ingredients such as proteins, vaccines, anticancer drugs and therapeutic nucleic acids can be loaded onto CNTs via non-specific interaction or covalent conjugation with high loading capability.[12, 13] These active agents can be effectively delivered to targeting sites and cells, which could therefore significantly improve the therapeutic profile of active agents and ease up their adverse effects.[12, 13] However, due to the strong interaction between individual CNTs, unmodified CNTs tend to intertwine into larger clusters and are difficult to be dispersed in aqueous solution. On the other hand, CNTs have demonstrated to be toxic to different living organisms and would be mainly accumulated in reticuloendothelial systems (RES) after intravenously administration.[14-20] It is therefore suitable surface functionalization of CNTs is crucial important for their biomedical applications.

Mussel inspired chemistry has being emerged as an attractive surface modification strategy since pioneering work by *Lee* et al in 2007.[21] Due to the universal and strong adhesion of polydopamine (PDA) to various materials regardless their compositions, shape, size and structure, mussel inspired chemistry has been extensively explored for different applications ranged from energy storage and conversion to environmental protection and biomedical applications *etc*.[22-39] For example, *Lee* and *Park et al* have demonstrated PDA can facilely deposite on various materials via mussel inspired chemistry. These PDA can further served as template for biomineralization to fabricate hydroxyapatite based organic-inorganic hybrid biomaterials.[23] Park *et al* also found that PDA functionalized polycaprolactone nanofiber exhibited highly enhanced adhesion and viability toward human umbilical vein endothelial cells as compared to unmodified and gelatin-coated nanofibers.[34] More recently, Lee *et al* confirmed that PDA coating could obviously attenuate the inflammatory and immunological responses to contact tissue or blood.[40] Although the underline mechanism for these results is still not defined, these prophase results suggested that PDA might be a promising platform for fabrication of biomaterials. More importantly, these PDA coating could further modified with other functional components via Michael addition reaction owing to a large number of reactive sites were existed on these PDA coating.[41-43] Therefore, more elegant multifunctional hybrid biomaterials could fabricate via mussel inspired chemistry.

Polyethylene glycol (PEG) is an amphiphilic polymer, which is non-toxic, water dispersible, biocompatibile, non-immunogenicity and non-inflammatory. It has been demonstrated

that the pharmacokinetic behavior of materials can be significantly improved after PEGylation.[44] Because of these advantages of PEG, PEGylation has been widely explored for surface modification of materials such as CNTs and nanodiamonds for biomedical applications.[44-49] Different strategies for PEGylation including non-covalent adsorption, covalent conjugation and surface polymerization have been developed. For example, Dai *et al* has demonstrated that amphiphilic PEG molecules could be adsorbed on CNTs through hydrophobic interaction between the CNTs and the hydrophobic segment of these functionalized PEG molecules.[50] These PEGylated CNTs showed high dispersibility in physiological solution, good biocompatibility and long blood circulation time.[51] As compared with the non-covalent strategy, PEGylation via surface polymerization is another important strategy for surface modification of CNTs due to its variability and designability.[45] However, PEGylation through surface polymerization should first introduce function groups on the surface CNTs, which is complexity, and requirement of hazardous chemical reagents.[52, 53] Therefore, a novel strategy for preparation of PEGylated CNTs is still high desirable. To the best of our knowledge, the surface PEGylation of CNTs via mussel inspired chemistry has not reported thus far.

In this contribution, a novel strategy for surface modification of CNTs has been reported via mussel inspired chemistry. As shown in Scheme 1, polyethylene glycol methyl ether methacrylate (PEGMA) and itaconic anhydride (IA) were first copolymerized using 2, 2-Azobisisobutyronitrile (AIBN) as radical initiator to obtain poly(PEGMA-co-IA) bearing with pendant IA via free radical polymerization. Then dopamine hydrochloride (DA) was reacted with the pendant IA of poly(PEGMA-co-IA) via ring opening reaction. The final polymer poly(PEGMA-co-IA-DA) with pendant DA could facilely linked with CNTs via mussel inspired method. The dispersibility as well as the biocompatibility of these PEGylated CNTs was further examined. We demonstrated that these PEGylated CNTs showed high dispersibility and good biocompatibility toward cancer cells. Given the strong and universal adhesion of PDA toward various materials, this method described in this work may provide a general platform for fabrication of biomaterials.

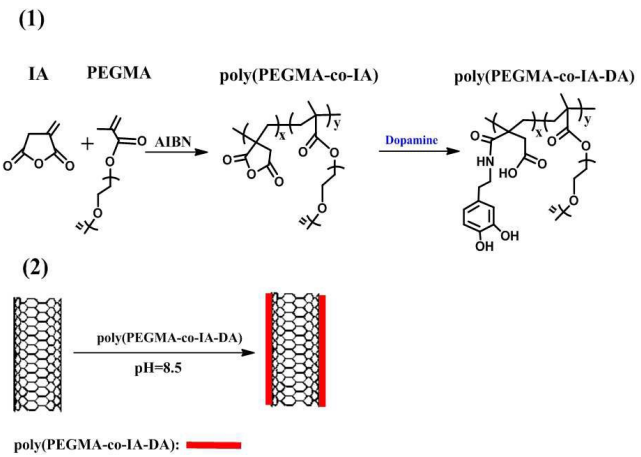

Scheme 1. Schematic illustration for the preparation of PEGMA-co-IA-DA functionalized CNT_S via mussel inspired chemistry. 1) First the monomers IA and PEGMA were copolymerized via free radical living polymerization using AIBN as the radical initiator at 80 °C for 24 h. Thus obtained copolymers named as poly(PEGMA-co-IA) were further reacted with dopamine through the ring opening reaction between the IA and the amino group of dopamine. 2) The finally polymers named as poly(PEGMA-co-IA-DA) were utilized for surface modification of CNTs via mussel inspired chemistry.

2 Experiment sections

2.1 Materials and instruments

All chemicals were of analytical grade and were used as received without any further purification. All aqueous solutions were prepared with distilled water. CNTs with diameter of 30-50 nm were purchased from sinonano (Beijing, China), dopamine hydrochloride (DA, MW:189.64 Da, >98%) were supplied from company of Sangon Biotech, Tris hydroxyl methyl aminomethan (Tris), poly(ethylene glycol) methyl ether methacrylate (PEGMA, MW:950 Da, 98%), itaconic anhydride (IA, MW:112.19 Da, 96%), 2,2-Azodiisobutyronitrile (AIBN, MW:164.21 Da, 98%) were purchased from Aladdin (Shanghai, China). Anhydrous ethyl acetate and methanol were offered by Heowns (Tianjin, China). All other solvents and chemicals were commercial available and used directly without any purification.

^{1}H NMR spectra were recorded on Bruker Avance-400 spectrometer with D_2O as the solvent. The synthetic polymers and materials were characterized by Fourier transform infrared spectroscopy (FT-IR) using KBr pellets. The Fourier transform infrared (FT-IR) spectra were supplied from Nicolet5700 (Thermo Nicolet corporation). Transmission electron microscopy (TEM) images were recorded on a Hitachi 7650B microscope operated at 80 kV, the TEM specimens were got by putting a drop of the nanoparticle ethanol suspension on a carbon-coated copper grid. Thermal gravimetric analysis (TGA) was conducted on a TA instrument Q50 with a heating rate of 20 °C min^{-1}. Samples weighing between 10 to 20 mg were heated from 25 to 500 °C in air flow (60 mL min^{-1}), N_2 as the balance gas (40 mL min^{-1}). Raman spectra of CNT nanoparticles were conducted on a RM 2000 microscopic confocal Raman spectrometer (Renishaw PLC, England) employing a 514.5 nm laser beam. The X-ray photoelectron spectra (XPS) were performed on a VGESCALAB 220-IXL spectrometer using an Al Kα X-ray source (1486.6 eV). The energy scale was internally calibrated by referencing to the binding energy of the C1s peak of a carbon contaminant at 284.6 eV. The size distribution of PEGylated CNT in water was determined using a zeta Plus apparatus (ZetaPlus, Brookhaven Instruments, Holtsville, NY). Each sample was ultrasonicated for 30 min prior to analysis.

2.2 Synthesis of poly(PEGMA-co-IA-DA)

The poly(PEGMA-co-IA) polymers could be synthesized via living free radical polymerization using PEGMA and IA as the monomers. The synthetic process was described as follow. The mixture of PEGMA (4 mM, 0.68 g), IA (1 mM, 0.12 g) and AIBN (2 mM, 0.33 g) were dissolved in anhydrous ethyl acetate solution (30 mL) and stirring at 80 °C for 24 h. The system was filled with dry N_2 and sealed. After 24 h, the DA dissolved in methanol was injected into sealed system and maintained for 2 h. The crude product was purified by dialysis against de-ionic water and ethanol for 2 days. The finally polymers were dried in a vacuum oven at 40 °C for 24 h.

2.3 Preparation of poly(PEGMA-co-IA-DA) functionalized CNTs

Poly(PEGMA-co-IA) modified the surface of CNTs via mussel inspired chemistry. 100 mg of CNTs were put into the 30 mL of Tris buffer solution (pH = 8.5) and ultrasonic treatment for 10 min. Afterword, poly(PEGMA-co-IA-DA) was dissolved in Tris buffer solution (pH = 8.5) and added into the CNTs. After stirring at room temperature for 12 h, CNT-poly(PEGMA-co-IA-DA) was separated by centrifugation at 8000 rpm for 10 min, the modified materials were washed and centrifuged three times using distilled water and dried at 50 °C for 12 h.

2.4 Biocompatibility evaluation of CNT-poly(PEGMA-co-IA-DA)

The biocompatibility of CNT-poly(PEGMA-co-IA-DA) composites to human hepatocellular carcinoma (HepG2) cells was first evaluated by cell morphology observation.[54, 55] Briefly, cells were seeded in 6-well microplates at a density of 1×10^5 cells per mL in 2 mL of the respective media containing 10% heat-inactivated fetal bovine serum (FBS). After cell attachment, plates were washed with phosphate buffer solution (PBS) and the cells were treated with complete cell culture medium, or different concentration of PEGylated CNTs prepared in 10% FBS containing media for 24 h. Then all samples were washed with PBS three times to remove the uninternalized CNTs. The morphology of cells was observed by an optical microscopy (Leica, Germany).

The cell viability was further used to quantitatively evaluate the biocompatibility of CNT-poly(PEGMA-co-IA-DA) using the WST assay as described in our previous reports.[56] Briefly, HepG2 cells and human alveolar basal epithelial (A549) cells were seeded in 96-well microplates at a density of 5×10^4 cells per mL in 160 μL of the respective media containing 10% FBS. After 24 h of cell attachment, the cells were incubated with 10, 20, 40, 80, 120 μg mL^{-1} of CNT-poly(PEGMA-co-IA-DA) for 12 and 24 h. Then the cells were washed with PBS for three times to remove the uninternalized nanoparticles. After that, 10 μL of CCK-8 dye and 100 μL of Dulbecco's Modified Eagle's Medium (DMEM) cell culture media was added to each well and incubated for 2 h at 37 °C. Plates were then analyzed with a microplate reader (VictorIII, Perkin-Elmer). Measurements of dye absorbance were carried out at 450 nm, with the reference wavelength at 620 nm. The values were proportional to the number of live cells. The percent reduction of WST was compared to the control (cells not exposed to nanoparticles), which represented 100% WST reduction. Three replicate wells were used for each control and test concentrations per microplate, and the experiment was repeated three times. Cell survival was expressed as absorbance relative to that of untreated controls. Results are presented as mean ± standard deviation (SD). As a comparison, the cell viability of pristine CNTs to HepG2 cells was also measured using the identified experimental conditions.

2.5 Reactive oxygen species (ROS) generation

ROS generation measurement was used to examine the oxidative stress induced by CNT-poly(PEGMA-co-IA-DA).[57] The ability of CNT-poly(PEGMA-co-IA-DA) to induce intracellular ROS formation was determined using a 2,7-dichlorodihydrofluorescein diacetate (DCFH-DA) assay as reported in our previous work.[58, 59] Briefly, A549 cells were cultured in 96 well plates and incubated with different concentrations (10, 20, 40, 80 and 120 μg mL^{-1}) of CNT-poly(PEGMA-co-IA-DA) for 24 h. After washed three times with PBS to remove the uninternalized nanoparticles, cells were subsequently incubated in 200 μL of a working solution of DCFH-DA, a fluorogenic probe commonly used to detect intracellular generation of ROS, at 37 °C for 30 min. Fluorescence data of oxidized DCFH-DA were recorded by using a microplate reader (VictorIII, Perkin-Elmer) with the excitation and emission wavelengths set at 485 and 535 nm, respectively. The fluorescence of cells without incubation with dyes was defined as the background (F_0), and cells incubated with 0.5 and 1.0 mg mL^{-1} of Rosup for 30 min served as the positive control. The values were expressed as a percentage of fluorescence intensity relative to control wells. All the procedures were performed without exposure to light. Three replicate wells were used for each control and test concentrations per microplate, and the experiment was repeated three times. Results are presented as mean ± SD.

3. Results and discussion

3.1 Characterization of polymers and CNTs

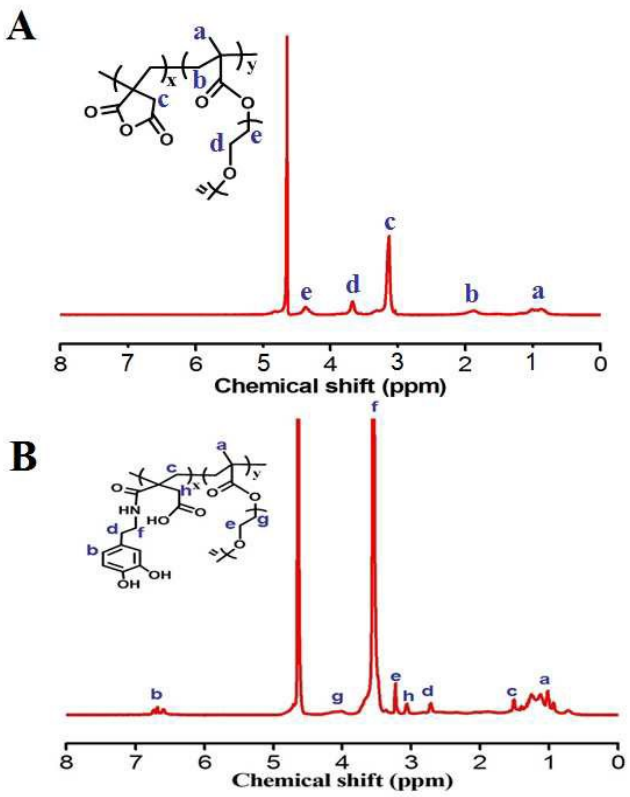

Fig. 1 ^{1}H NMR spectra of (A) poly(PEGMA-co-IA) and (B) poly(PEGMA-co-IA-DA) using D_2O as solvent.

The successful preparation of PEGMA-co-IA and PEGMA-co-IA-DA copolymers was confirmed by ^{1}H NMR spectroscopy. As shown in Fig. 1, the structure of PEGMA-co-IA and PEGMA-co-IA-DA copolymers could be decided by ^{1}H NMR (D_2O) spectra. The results of ^{1}H NMR described as following. According to the

Fig. 1A, the peaks at δ= 0.9-1.2 ppm (-CH_3), δ= 1.8-2.0 ppm (-CH_2-CH_2), δ= 3.15 ppm (-CO-CH_2), δ= 3.67 ppm (O-CH_2) and δ= 4.37 ppm (-COO-CH_2) could contribute to PEGMA-co-IA polymer. Fig. 1B also shows that the PEGMA-co-IA-DA polymer was successfully synthesized via ring-opening reaction. Different peaks belong to PEGMA-co-IA-DA polymer could be summarized as follows: δ= 1.13 ppm (-CH_3), δ= 1.50 ppm (-CH_2-CH_2-), δ= 2.71 ppm (Ph-$\underline{CH_2}$), δ= 3.06 ppm (-CO-CH_2), δ= 3.32 ppm (-O-CH_2), δ= 3.54 ppm (NH-$\underline{CH_2}$), δ= 4.02 ppm (-COO-CH_2) and δ= 6.68 ppm (C_6H_5-).

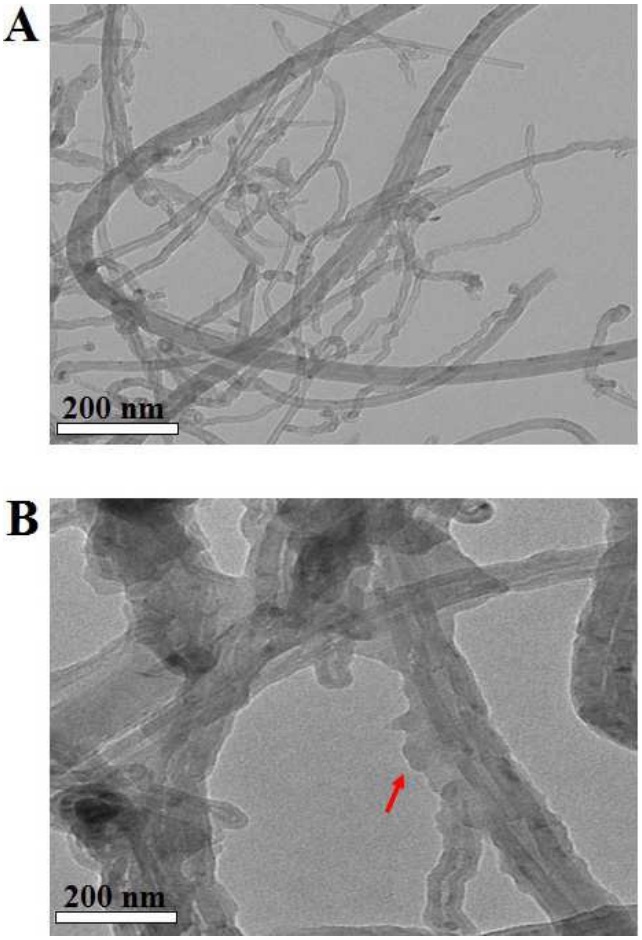

Fig. 2 Representative TEM images of CNTs (A) and CNT-poly(PEGMA-co-IA-DA) (B). As evidenced by TEM images, the diameter of pristine CNTs is 30-50 nm. Scale bar = 200 nm. After surface modification with polymers, obvious thin film coated on CNTs can be identified, indicating that CNTs were functionalized with polymers.

Fig. 2 shows the representative TEM images of pristine CNTs and CNT-poly(PEGMA-co-IA-DA). As evidenced by Fig. 2A, the diameter of CNTs is 30-50 nm, which is well consistent with production information provided by manufacturer. As compared with the pristine CNTs, however, after modifying CNTs surface with poly(PEGMA-co-IA-DA), the structure of CNTs remains intact (Fig. 2B), which indicates the properties of CNTs related to their structure are preserved. As showed in Fig. 2B, some polymer films coated on the CNTs was observed after drastically removing free poly(PEGMA-co-IA-DA) by washing thoroughly with water and acetone. Based on the TEM images, the thickness of polymer films is ranged about 10-17 nm. These results suggested that poly(PEGMA-co-IA-DA) can be successfully and firmly functionalized with CNTs via mussel inspired chemistry.

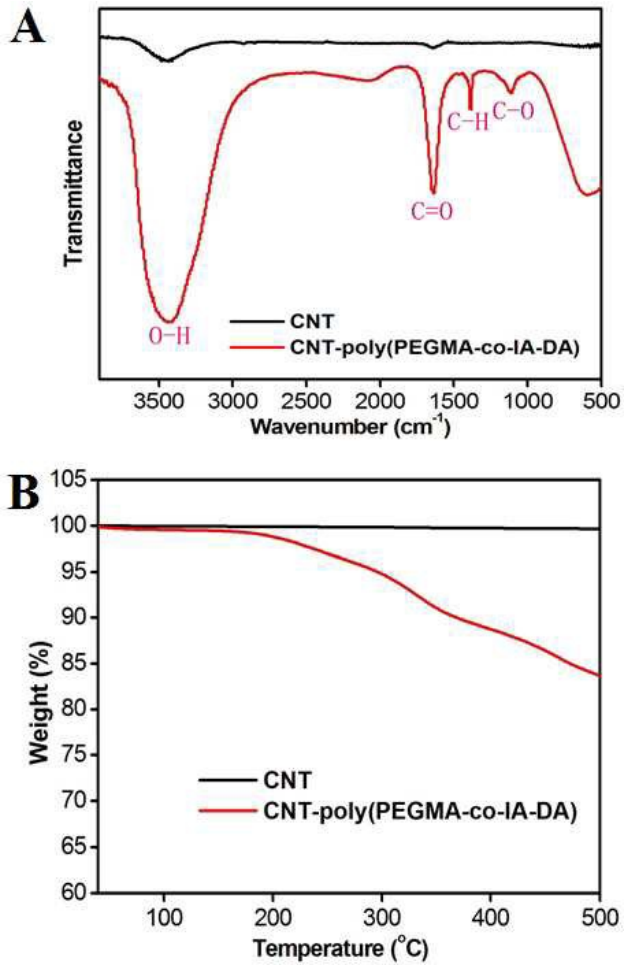

Fig. 3 (A) FT-IR spectra of CNTs and CNT-poly(PEGMA-co-IA-DA), (B) TGA curves of CNTs and CNT-poly(PEGMA-co-IA-DA)

The functional groups that existed on the surface of CNTs before and after modification were characterized by FT-IR spectroscopy. Three characteristic peaks were observed from Fig. 3A, the characteristic peaks from pure CNTs were not appeared at 1709 cm^{-1} and 3656 cm^{-1}, but after introducing poly(PEGMA-co-IA-DA) onto the surface of CNTs, the intensity of absorption at 3656 cm^{-1} (-OH), 1741 cm^{-1} (-$\underline{CO}$-OH) and 1116 cm^{-1} (C-O-C) was significantly improved, indicating that C-O-C, -COOH and -OH functional groups were introduced on the surface of CNTs via mussel inspired chemistry. Furthermore, the characteristic peak of C-H bending vibration appears at 1430 cm^{-1}, also indicating that poly(PEGMA-co-IA) was coated on CNTs. Fig. 3B shows that the TGA curves of CNTs and CNT-poly(PEGMA-co-IA-DA). The weight loss percentages of pure CNTs were 2.7% at 500 °C, suggesting that excellent thermal stability of CNTs. However, the weight loss of CNT-poly(PEGMA-co-IA-DA) was significantly increased to 25% under the sample experiment condition, implying that poly(PEGMA-co-IA-DA) was successfully introduced onto the surface of CNTs via mussel inspired chemistry. The major weight loss of CNT-poly(PEGMA-co-IA-DA) happened between 195 °C to 499 °C.[60] TGA results suggest that poly(PEGMA-co-IA-DA)

was absolutely decomposed at 500 °C. Thus the grafting ratio of poly(PEGMA-co-IA-DA) on CNTs is about 22.3%. The raman spectrum of CNT-poly(PEGMA-co-IA-DA) was displayed in Fig. S1. Two characteristic Raman peaks were observed, which were located at 1342.6 and 1577.6 cm^{-1}. The two Ramn peaks could be assigned to the D and G bands of CNT-poly(PEGMA-co-IA-DA), respectively. Based on the Raman spectrum, the ratio of D/G was increased to 0.72, which is much greater than that of the prisitine CNTs. The Raman spectrum further implied the successful modification of CNTs with poly(PEGMA-co-IA-DA).

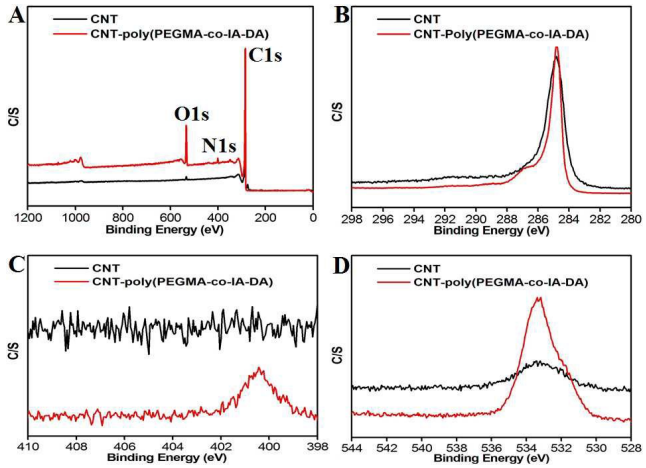

Fig. 4 XPS spectra of CNTs and CNT-poly(PEGMA-co-IA-DA). (A) The Survey scan the spectral region from 0 to 1200 eV, (B) The C1s region, (C) The N1s region, and (D) The O1s region.

A survey of XPS scan ranging from 0 to 1200 eV was appeared to detect the elements present in the different CNTs samples. As shown in Fig. 4A, XPS survey of these samples revealed the existence of C, N and O elements. The high resolution C1s, O1s and N1s XPS spectra were shown from Fig. 4B-D. A broad peak between 284 and 286 eV shows overlap of two different binding energy of carbon (Fig. 4B). The broad peak at 285 eV originates from sp^3-hybridised carbon atoms. The higher binding energy signal appeared at 287 eV can be attributed to the carbon atoms bound to oxygen (Fig. 4B). Furthermore, a novel peak referred to N1s at 400.4 eV was emerged in the sample of CNT-poly(PEGMA-co-IA-DA), confirming the successful modification of CNTs with poly(PEGMA-co-IA-DA) (Fig. 4C). Fig. 4D shows the O1s XPS spectra of CNTs. It can be seen that the O1s spectra of CNT-poly(PEGMA-co-IA-DA) with binding energy centered at 533 eV can be observed. As compared with the pristine CNTs, the intensity of N1s and O1s was significantly increased after modification with poly(PEGMA-co-IA-DA). The XPS results further confirmed the successful modification of poly(PEGMA-co-IA-DA) with CNTs.

Table 1

Element content (%) of CNTs and CNT-poly(PEGMA-co-IA-DA) based on the XPS analysis

	C1s	O1s	N1s
CNTs	97.13	2.87	0
CNT-poly(PEGMA-co-IA-DA)	87.87	10.34	1.79

Based on the XPS spectra, the element concentrations of C, N and O were calculated and listed in Table 1. The concentration of C atom for CNTs was about 97.13%. However, the concentration of C was decreased to 87.87% in the sample of CNT-poly(PEGMA-co-IA-DA). On the contrary, the concentration of O atom was increased from 2.87% (CNTs) to 10.34% (CNT-poly(PEGMA-co-IA-DA)). Furthermore, the new N atom was introduced into the materials with percentage of 1.79%. The results from XPS spectra are similar to the TGA results, providing further evidence that poly(PEGMA-co-IA) was conjugated on the surface of CNTs.

3.2 Dispersibility of CNTs

The dispersibility of pristine and CNT-poly(PEGMA-co-IA-DA) in water and organic solvents was further determined and showed in Fig. 5. It can be seen that the water dispersibility of CNT-poly(PEGMA-co-IA-DA) is obviously improved as compared with the pristine CNTs. As shown in Fig. 5A, the pristine CNTs have been quickly precipitated (left bottle in Fig. 5A). However, CNT-poly(PEGMA-co-IA-DA) still well dispersed in water after 24 h deposition. These results also implied that poly(PEGMA-co-IA-DA) was successfully conjugated on CNTs. On the other hand, the dispersion of CNT-poly(PEGMA-co-IA-DA) in other organic solvents was also evaluated. It can be seen that CNT-poly(PEGMA-co-IA-DA) shows excellent dispersibility in dimethyl sulfoxide (DMSO) and tetrahydrofuran (THF) for more than 12 h. The hydrodynamic size of CNT-poly(PEGMA-co-IA-DA) was further examined by dynamic laser scattering (DLS). As shown in Fig. S2A, the size distribution of CNT-poly(PEGMA-co-IA-DA) is 109.9 ± 41.2 nm with narrow size distribution (polydispersity index is 0.232). On the other hand, the dispersibility of CNT-poly(PEGMA-co-IA-DA) in physiological solution was also investigated. As shown in Fig. S2, no obvious aggregation was observed in the upper cuvette (in PBS) and below cuvette (in DMEM) after the CNT-poly(PEGMA-co-IA-DA) suspensions were deposited for 2 h, implying their good dispersibility in PBS and cell culture medium. The hydrodynamic size distribution of CNT-poly(PEGMA-co-IA-DA) in PBS and DMEM cell culture medium was also measured. Results showed that the size distribution of CNT-poly(PEGMA-co-IA-DA) in PBS and DMEM is 314.1 ± 140.7 nm and 529.3 ± 32.3 nm, respectively (Fig. S2B and Fig. S2C). These results suggested that CNT-poly(PEGMA-co-IA-DA) can be well dispersed in physiological solution. Given the excellent water dispersibility, the biocompatibility of CNTs-poly(PEGMA-co-IA-DA) was subsequently investigated.

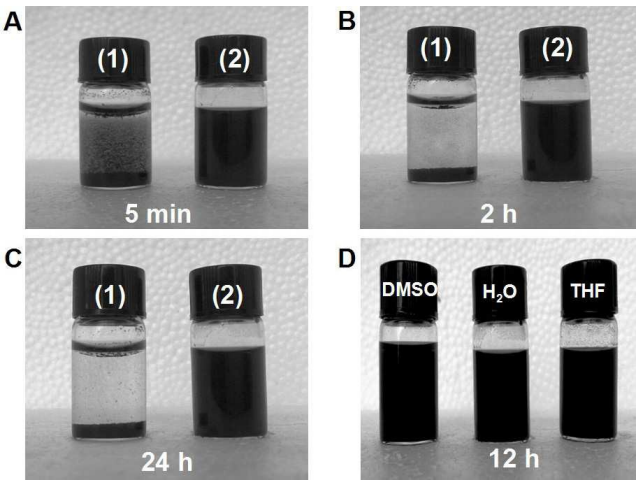

Fig. 5 Photographs of CNTs (1) and CNT-poly(PEGMA-co-IA-DA) (2) in water for different time points (A) 5 min, (B) 2 h and (C) 24 h. (D) Dispersibility of CNT-poly(PEGMA-co-IA-DA) in different solution including DMSO, H_2O and THF.

3.3 Cell viability evaluation of CNT-poly(PEGMA-co-IA-DA)

The biocompatibility of CNT-poly(PEGMA-co-IA-DA) was first examined by optical microscopy observation. Fig. S3 shows the optical microscopy images of HepG2 cells, which were incubated with different concentrations of CNT-poly(PEGMA-co-IA-DA) for 24 h. It can be seen that cells were still adhered to cell plate very well as compared with the control cells. Even the concentration of CNT-poly(PEGMA-co-IA-DA) is as high as 80 μg mL^{-1}, no obvious cell morphology change and cell number decrease was observed. The optical microscopy observation results implying the good cytocompatibility of CNT-poly(PEGMA-co-IA-DA).

The cell viability of CNT-poly(PEGMA-co-IA-DA) toward HepG2 and A549 cells cells was further evaluated using CCK-8 assay. As shown in Fig. 6A, cell viability of HepG2 cells is almost no significant decrease after cells were incubated with different concentrations of CNT-poly(PEGMA-co-IA-DA) for 12 and 24 h. Even the concentration of CNT-poly(PEGMA-co-IA-DA) is 120 μg mL^{-1}, the cell viability value is still greater than 90%. The half maximal inhibitory concentration (IC50) value of CNT-poly(PEGMA-co-IA-DA) to HepG2 calculated from Fig. 6A is about 549.3 μg mL^{-1}. The cell viability of CNT-poly(PEGMA-co-IA-DA) to A549 cells was also examined. Results suggested that CNT-poly(PEGMA-co-IA-DA) are also biocompatibility with A549 cells. The IC50 value of CNT-poly(PEGMA-co-IA-DA) to A549 is 213.3 μg mL^{-1}. These results confirmed that CNT-poly(PEGMA-co-IA-DA) are biocompatible with cancer cells. On the other hand, the effect of pristine CNTs on the HepG2 cells was also evaluated using CCK-8 assay. Results showed that obvious cytotoxicity was observed based on the cell viability values. It can be seen that the cell viability is about 71.6% and 58.5% after cells were incubated with 120 μg mL^{-1} for 12 and 24 h, respectively (Fig. S4). Based on the cell viability results, the IC50 of pristine CNTs to HepG2 cells at 24 h is about 175 μg mL^{-1}. These results suggested that the CNTs showed enhanced biocompatibility as compared with the pristine CNTs. The effect of surface modification on the biocompatibility of nanomaterials was also found by some previous reports. For example, Zhu et al have investigated the effect of proteins on the cytotoxicity of carbon nanomaterials. They demonstrated that the CNTs showed less cytotoxicity in the serum contained cell culture medium than in serum free cell culture medium.[61, 62] The surface treatment could also influence the biocompatibility of CNTs. It has been demonstrated that the anneal CNTs (CNTan) showed better biocompatibility as compared with the oxidant CNTs (CNTox).[53] PEGylation is an important surface modification strategy for biomedical applications of nanomaterials. It has been demonstrated that PEGylation could not only improve the water dispersibility of nanomaterials, but also change their pharmacokinetic behavior.[63, 64] Therefore, development of general and facile PEGylation strategies is of great research interest for the biomedical applications of nanomaterials.

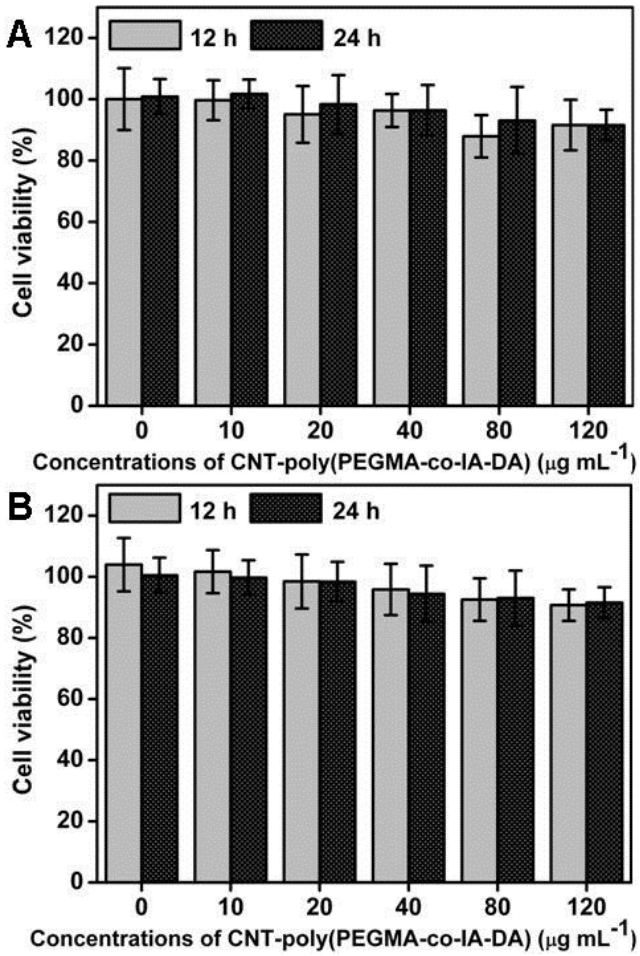

Fig. 6 Cytotoxicity of CNT-poly(PEGMA-co-IA-DA) with (A) HepG2 cells and (B) A549 cells for 12 and 24 h. The concentration of CNT-poly(PEGMA-co-IA-DA) was ranged from 0-120 μg mL^{-1}.

3.4 ROS generation of CNT-poly(PEGMA-co-IA-DA)

It has been reported that cytotoxicity of many nanomaterials is associated with generation of ROS. Therefore, the ROS generation after cells incubated with different concentrations of CNT-poly(PEGMA-co-IA-DA) was further determined to understand the cytotoxicity mechanism. As shown in Fig. 7A, no obvious ROS increase was found as compared with the control cells. However, the positive control (cells incubated with Rosup

for 30 min) showed almost 7.5 folds increase of fluorescent intensity (Fig. 7B). These results further confirmed the excellent biocompatibility of CNT-poly(PEGMA-co-IA-DA). The biocompatibility of CNTs has been intensively investigated previously. It has been demonstrated that the cytotoxicity of CNTs are related to a number of factors such as physciochemical properties of CNTs (transition metal catalyst, surface chemistry and water dispersiblity) and components of cell culture medium (proteins, phenol red and essential micronutrients).[61, 65-68] Very surprisingly, we found that the ROS was decreased in some extent after cells were incubated with CNT-poly(PEGMA-co-IA-DA), which is significantly different from many previous reports.[52] The possible mechanism for the decrease of ROS could be ascribed to the following reasons. First, polymers coated on CNTs can effective impede the cell uptake of CNTs, leading to the acute exposure dosage of CNTs is relative low. Second, it has been reported the PDA could eliminate the free radical from cells, thus protecting cells injured by CNTs.[69] Given the high water dispersiblity and excellent biocompatibility, CNT-poly(PEGMA-co-IA-DA) are expected very suitable for biomedical applications.

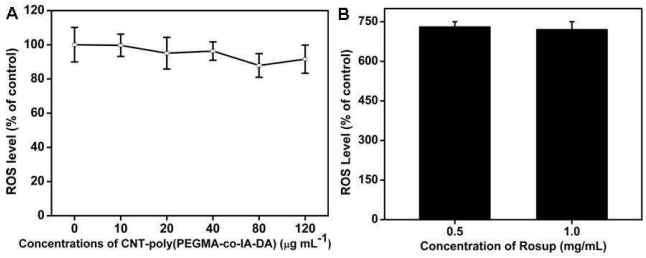

Fig. 7 ROS generation of cells after they were incubated with different concentrations of CNT-poly(PEGMA-co-IA-DA) for 24 h (A) and ROS generation of cells after they were incubated with 0.5 and 1 mg mL^{-1} of Rosup for 30 min (B).

4. Conclusions

In this work, the successful functionalization of CNTs with water soluble and biocompatible polymers (poly(PEGMA-co-IA-DA)) was reported for the first time. These PEGylated CNTs exhibited high water dispersibility and excellent biocompatibility, making them high potential for biomedical applications. The method described in this work is rather simple, effective and universal. Apart from CNTs, it can also be utilized for surface modification of almost any materials and surface due to the strong and universal adhesion of PDA. We therefore expected that this strategy will provide a general platform for fabrication of different biomaterials for biomedical applications.

Acknowledgements

This research was supported by the National Science Foundation of China (Nos. 21104039, 21134004, 21201108, 21474057), and the National 973 Project (Nos. 2011CB935700).

Notes

[a] Department of Chemistry, Nanchang University, 999 Xuefu Avenue, Nanchang 330031, China. [b] Department of Chemistry and the Tsinghua Center for Frontier Polymer Research, Tsinghua University, Beijing, 100084, P. R. China.
fengjiedeng@aliyun.com;xiaoyongzhang1980@gmail.com; weiyen@tsinghua.edu.cn.

† Electronic Supplementary Information (ESI) available: [Raman spectroscopy characterization, hydrodynamic size of CNT-poly(PEGMA-co-IA-DA), optical microscopy observation of cells were provided in supplementary information]. See DOI: 10.1039/b000000x/

References

1. S. Iijima, *Nature*, 1991, **354**, 56-58.
2. H.-M. Cheng, Q.-H. Yang and C. Liu, *Carbon*, 2001, **39**, 1447-1454.
3. X. Liu, L. Guo, D. Morris, A. B. Kane and R. H. Hurt, *Carbon*, 2008, **46**, 489-500.
4. S. Ravindran, S. Chaudhary, B. Colburn, M. Ozkan and C. S. Ozkan, *Nano Lett.*, 2003, **3**, 447-453.
5. M. Anantram and F. Leonard, *Rep. Prog. Phys.* , 2006, **69**, 507-561.
6. S. M. Lee and Y. H. Lee, *Appl. Phys. Lett.*, 2000, **76**, 2877-2879.
7. E. Munoz-Sandoval, N. Perea-Lopez, R. Lima-Juarez, G. J. Labrada-Delgado, B. A. Rivera-Escoto, A. Zamudio, H. G. Silva-Pereyra, E. Robles-Avila and M. Terrones, *Carbon*, 2014, **77**, 722-737.
8. J. Zhu, N. Jia, J. Park and K. Gong, *Carbon*, 2013, **61**, 270-277.
9. X. Geng, F. Li, D.-w. Wang and H.-m. Cheng, *Carbon*, 2013, **60**, 564.
10. N. W. Shi Kam, T. C. Jessop, P. A. Wender and H. Dai, *J. Am. Chem. Soc.*, 2004, **126**, 6850-6851.
11. N. W. S. Kam, Z. Liu and H. Dai, *Angew. Chem. Int. Ed*, 2006, **118**, 591-595.
12. N. W. S. Kam, M. O'Connell, J. A. Wisdom and H. Dai, *P. Natl. Acad. Sci.*, 2005, **102**, 11600-11605.
13. Z. Liu, C. Davis, W. Cai, L. He, X. Chen and H. Dai, *P. Natl. Acad. Sci.*, 2008, **105**, 1410-1415.
14. Z. Li, Y. Geng, X. Zhang, W. Qi, Q. Fan, Y. Li, Z. Jiao, J. Wang, Y. Tang and X. Duan, *J. Nanopart. Res.*, 2011, **13**, 2939-2947.
15. H. Wang, J. Wang, X. Deng, H. Sun, Z. Shi, Z. Gu, Y. Liu and Y. Zhaoc, *J. Nanosci. Nanotechno.*, 2004, **4**, 1019-1024.
16. Y. Liu, Y. Zhao, B. Sun and C. Chen, *Acc. Chem. Res.*, 2012, **46**, 702-713.
17. G. Jia, H. Wang, L. Yan, X. Wang, R. Pei, T. Yan, Y. Zhao and X. Guo, *Environ. Sci. Technol.*, 2005, **39**, 1378-1383.
18. L. Meng, R. Chen, A. Jiang, L. Wang, P. Wang, C. Li, R. Bai, Y. Zhao, H. Autrup and C. Chen, *Small*, 2013, **9**, 1786-1798.
19. X. Deng, S. Yang, H. Nie, H. Wang and Y. Liu, *Nanotechnology*, 2008, **19**, 075101.
20. Z. Lin, Z. Xi and J. Huang, *Toxicol. Res.*, 2014, 10.1039/C1033TX50059D.
21. H. Lee, S. M. Dellatore, W. M. Miller and P. B. Messersmith, *Science*, 2007, **318**, 426-430.
22. Y. Liu, B. Yu, J. Hao and F. Zhou, *J. Colloid Interf. Sci.* , 2011, **362**, 127-134.
23. J. Ryu, S. H. Ku, H. Lee and C. B. Park, *Adv. Funct. Mater.*, 2010, **20**, 2132-2139.
24. H. Hu, B. Yu, Q. Ye, Y. Gu and F. Zhou, *Carbon*, 2010, **48**, 2347-2353.
25. S. M. Kang, S. Park, D. Kim, S. Y. Park, R. S. Ruoff and H. Lee, *Adv. Funct. Mater.*, 2011, **21**, 108-112.
26. B. Fei, B. Qian, Z. Yang, R. Wang, W. Liu, C. Mak and J. H. Xin, *Carbon*, 2008, **46**, 1795-1797.
27. W. Lee, J. U. Lee, B. M. Jung, J.-H. Byun, J.-W. Yi, S.-B. Lee and B.-S. Kim, *Carbon*, 2013, **65**, 296-304.
28. D. E. Fullenkamp, J. Rivera, Y.-k. Gong, K. Lau, L. He, R. Varshney and P. B. Messersmith, *Biomaterials*, 2012, **33**, 3783-3791.
29. Y. Lee, H. Lee, Y. B. Kim, J. Kim, T. Hyeon, H. Park, P. B. Messersmith and T. G. Park, *Adv. Mater.*, 2008, **20**, 4154-4157.
30. L. Xu, N. Liu, Y. Cao, F. Lu, Y. Chen, X. Zhang, L. Feng and Y. Wei, *ACS Appl. Mater. Interfaces*, 2014, **6**, 13324-13329.
31. Y. Liu, K. Ai and L. Lu, *Chem. Rev.*, 2014, DOI: 10.1021/cr400407a.
32. Q. Ye, F. Zhou and W. Liu, *Chem. Soc. Rev.*, 2011, **40**, 4244-4258.
33. M.-H. Ryou, Y. M. Lee, J.-K. Park and J. W. Choi, *Adv. Mater.*, 2011, **23**, 3066-3070.
34. S. H. Ku and C. B. Park, *Biomaterials*, 2010, **31**, 9431-9437.

35. X. Song, L. Lin, M. Rong, Y. Wang, Z. Xie and X. Chen, *Carbon*, 2014.
36. K. Ai, Y. Liu, C. Ruan, L. Lu and G. M. Lu, *Adv. Mater.*, 2013, **25**, 998-1003.
37. X. Zhang, S. Wang, L. Xu, Y. Ji, L. Feng, L. Tao, S. Li and Y. Wei, *Nanoscale*, 2012, **4**, 5581-5584.
38. Y. Liu, K. Ai, J. Liu, M. Deng, Y. He and L. Lu, *Adv. Mater.*, 2013, **25**, 1353-1359.
39. Q. Wan, M. Liu, J. Tian, F. Deng, G. Zeng, Z. Li, K. Wang, Q. Zhang, X. Zhang and Y. Wei, *Polym. Chem.*, 2015, **6**, 1786-1792.
40. S. Hong, K. Y. Kim, H. J. Wook, S. Y. Park, K. D. Lee, D. Y. Lee and H. Lee, *Nanomedicine*, 2011, **6**, 793-801.
41. Y. Cao, X. Zhang, L. Tao, K. Li, Z. Xue, L. Feng and Y. Wei, *ACS Appl. Mater. Inter.*, 2013, **5**, 4438-4442.
42. H. Lee, J. Rho and P. B. Messersmith, *Adv. Mater.*, 2009, **21**, 431-434.
43. L. Q. Xu, W. J. Yang, K.-G. Neoh, E.-T. Kang and G. D. Fu, *Macromolecules*, 2010, **43**, 8336-8339.
44. S.-T. Yang, K. Fernando, J.-H. Liu, J. Wang, H.-F. Sun, Y. Liu, M. Chen, Y. Huang, X. Wang and H. Wang, *Small*, 2008, **4**, 940-944.
45. X. Zhang, C. Fu, L. Feng, Y. Ji, L. Tao, Q. Huang, S. Li and Y. Wei, *Polymer*, 2012, **53**, 3178-3184.
46. X. Zhang, X. Zhang, B. Yang, J. Hui, M. Liu, W. Liu, Y. Chen and Y. Wei, *Polym. Chem.*, 2014, **5**, 689-693.
47. X. Zhang, X. Zhang, B. Yang, M. Liu, W. Liu, Y. Chen and Y. Wei, *Polym. Chem.*, 2014, **5**, 356-360.
48. X. Zhang, J. Hui, B. Yang, Y. Yang, D. Fan, M. Liu, L. Tao and Y. Wei, *Polym. Chem.*, 2013, **4**, 4120-4125.
49. X. Zhang, X. Zhang, B. Yang, S. Wang, M. Liu, Y. Zhang, L. Tao and Y. Wei, *RSC Adv.*, 2013, **3**, 9633-9636.
50. X. Zhang, S. Wang, C. Fu, L. Feng, Y. Ji, L. Tao, S. Li and Y. Wei, *Polym. Chem.*, 2012, **3**, 2716-2719.
51. Z. Liu, W. Cai, L. He, N. Nakayama, K. Chen, X. Sun, X. Chen and H. Dai, *Nat. Nanotech.*, 2006, **2**, 47-52.
52. X. Zhang, W. Hu, J. Li, L. Tao and Y. Wei, *Toxicol. Res.*, 2012, **1**, 62-68.
53. X. Zhang, Y. Zhu, J. Li, Z. Zhu, J. Li, W. Li and Q. Huang, *J. Nanopart. Res.*, 2011, **13**, 6941-6952.
54. X. Zhang, J. Yin, C. Peng, W. Hu, Z. Zhu, W. Li, C. Fan and Q. Huang, *Carbon*, 2011, **49**, 986-995.
55. L. Xu, X. Zhang, C. Zhu, Y. Zhang, C. Fu, B. Yang, L. Tao and Y. Wei, *J. Biomater. Sci-Polym E*, 2013, **24**, 1564-1574.
56. X. Zhang, S. Wang, M. Liu, J. Hui, B. Yang, L. Tao and Y. Wei, *Toxicol. Res.*, 2013, **2**, 335-346.
57. J. Yin, C. Kang, Y. Li, Q. Li, X. Zhang and W. Li, *Toxicol. Res.*, 2014, **3**, 367-374.
58. H. Qi, M. Liu, L. Xu, L. Feng, l. Tao, Y. Ji, X. Zhang and Y. Wei, *Toxicol. Res.*, 2013, **2**, 427-433.
59. X. Zhang, S. Wang, C. Fu, L. Feng, Y. Ji, L. Tao, S. Li and Y. Wei, *Polym. Chem.*, 2012, **3**, 2716-2719.
60. X. Zhang, S. Wang, C. Zhu, M. Liu, Y. Ji, L. Feng, L. Tao and Y. Wei, *J. Colloid Interf. Sci.*, 2011, **397**, 39-44.
61. Y. Zhu, W. Li, Q. Li, Y. Li, Y. Li, X. Zhang and Q. Huang, *Carbon*, 2009, **47**, 1351-1358.
62. J. Li, Y. Zhu, W. Li, X. Zhang, Y. Peng and Q. Huang, *Biomaterials*, 2010, **31**, 8410-8418.
63. X. Zhang, X. Zhang, B. Yang, Y. Zhang, M. Liu, W. Liu, Y. Chen and Y. Wei, *Colloids Surf. B Biointerfaces*, 2014, **113**, 435-441.
64. H. Li, X. Zhang, X. Zhang, B. Yang and Y. Wei, *Colloids Surf. B Biointerfaces*, 2014, **121**, 347-353.
65. C. Ge, J. Du, L. Zhao, L. Wang, Y. Liu, D. Li, Y. Yang, R. Zhou, Y. Zhao and Z. Chai, *P. Natl. Acad. Sci.*, 2011, **108**, 16968-16973.
66. Y. Zhu, X. Zhang, J. Zhu, Q. Zhao, Y. Li, W. Li, C. Fan and Q. Huang, *Int. J. Mol. Sci.*, 2012, **13**, 12336-12348.
67. L. Guo, A. Von Dem Bussche, M. Buechner, A. Yan, A. B. Kane and R. H. Hurt, *Small*, 2008, **4**, 721-727.
68. X. Zhang, M. Liu, X. Zhang, F. Deng, C. Zhou, J. Hui, W. Liu and Y. Wei, *Toxicol. Res.*, 2015, **4**, 160-168.
69. K.-Y. Ju, Y. Lee, S. Lee, S. B. Park and J.-K. Lee, *Biomacromolecules*, 2011, **12**, 625-632.